28th ITS World Congress, Los Angeles, USA, 18-22 September 2022

Paper ID 917

Conflict charts: effective design tools for cooperative driving strategies

Hao M. Wang[1*], Sergei S. Avedisov[2], Ahmed H. Sakr[3 a], Onur Altintas[2], Gábor Orosz[1,4]

1. Department of Mechanical Engineering, University of Michigan, MI 48109, USA ([*] haowangm@umich.edu)

2. Toyota Motor North America R&D – InfoTech Labs, Mountain View, CA 94043, USA

3. Department of Electrical and Computer Engineering, University of Windsor, ON, N9B 3P4, Canada

4. Department of Civil and Environmental Engineering, University of Michigan, MI 48109, USA

Abstract

In this paper, we showcase the applicability of conflict charts for cooperative driving in a scenario where an ego vehicle merges to a carriageway from an on-ramp while a remote vehicle approaches on the main road. We also demonstrate how conflict charts can be used for interpreting the information contained in wireless messages exchanged by connected vehicles to resolve conflicts in cooperative driving. We use the developed conflict charts to design a decision making and control strategy for the ego vehicle that maximizes its time efficiency while guaranteeing a conflict-free maneuver. Our results show the effectiveness of the conflict charts-based strategy using numerical simulations with real highway data.

Keywords:

Connectivity, Conflict analysis

1. Introduction

Maneuvers of road users may involve conflicts when their trajectories cross each other and they may appear at the same location at the same time. Such conflicts commonly appear in merges, roundabouts, unprotected left turns, and intersections. Mismanaging conflicts may compromise safety and cause accidents. Assuming all vehicles are connected and highly automated, existing research results have shown benefits of vehicle-to-everything (V2X) communication to improve safety and efficiency [1], [2]. In particular, connected automated vehicles may seek agreements about their future maneuvers via V2X [3]-[5], and then a large variety of methods can be used for decision making, motion planning and control [6]-[8]. However, for the next few decades, it is reasonable to expect mixed traffic environments with vehicles of different automation and cooperation levels (including human drivers) [9]-[11]. Finding systematic ways of resolving conflicts in such mixed environment then becomes a necessity.

In our recent work [12], we proposed a tool called conflict analysis using formal logic. Conflict analysis studies cooperative maneuvering between road users with different automation levels, and calculates the so-called no-conflict, conflict, and uncertain domains in the state space. The corresponding conflict charts can enable fast and reliable decision making and control design. In this paper, we propose an on-board decision making and control strategy that utilizes conflict charts to minimize the conservatism in

[a] Ahmed H. Sakr was with affiliation 2 during the time when the results were generated.

decision making and in the meantime guarantee a conflict-free maneuver. This way we demonstrate that conflict charts provide effective design tools for cooperative driving strategies.

We study conflicts between two vehicles where both vehicles are equipped with V2X connectivity. Fig. 1(a)-(c) show three different maneuvers, where the ego vehicle (white) merges ahead of, merges behind, and has a conflict with the remote vehicle (blue), respectively. We define a conflict zone of finite size, representing a safety buffer between vehicles where the shape and size may vary based on road configurations. In the merge maneuver, we consider this zone to be at rectangular shape fixed to the ground around the end of the ramp; see the red shaded area in Fig. 1. To prevent conflict, the two vehicles must not be present in the conflict zone at the same time.

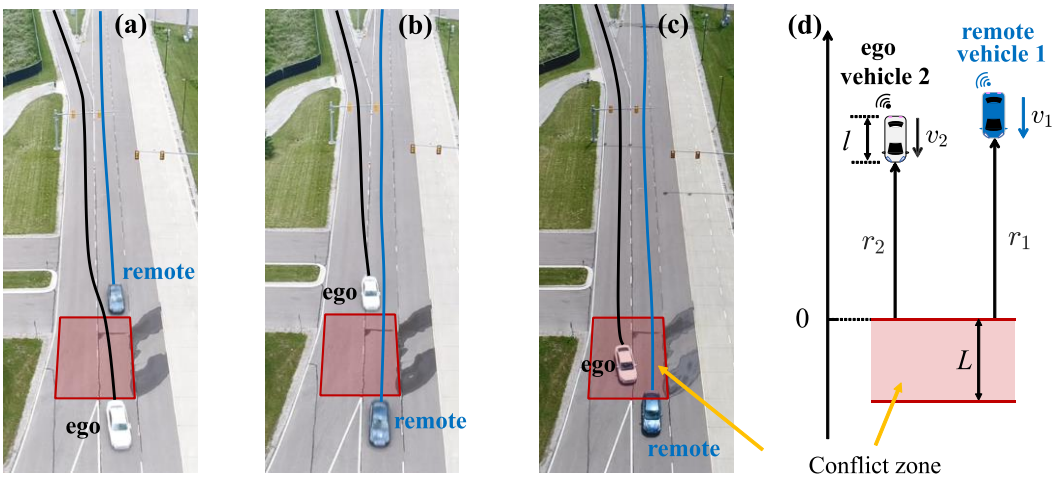

Fig. 1. - Two vehicles with potential conflict. (a) the ego vehicle merges ahead without conflict, (b) the ego vehicle merges behind without conflict, and (c) a conflict happens; (d) the generalized model of cooperative maneuvering. The red-shaded region indicates the conflict zone.

We resolve conflicts from the perspective of the ego vehicle because it must yield to the remote vehicle that is traveling on the main road according to the traffic rules. We consider that the ego vehicle receives V2X messages from the remote vehicle which contain the current status of the vehicle (e.g., GPS position and speed). One example of standardized status sharing messages is the basic safety message (BSM) [13]. By observing the conflict charts, we propose a strategy for the ego vehicle, which enables real-time decision making whether it should merge ahead of or behind the remote vehicle. Moreover, the proposed control algorithm maximizes the ego vehicle's chance to merge ahead while ensuring non-conflicting merge. These benefits are demonstrated via numerical simulations using traffic data taken on a highway in south-east Michigan.

2. Modeling vehicle dynamics

Consider the scenarios shown in Fig. 1(a)-(c) where the ego vehicle 2 (white) is joining the main carriageway from an on-ramp while the remote vehicle 1 (blue) is approaching along the main road. The conflict zone is located towards the end of the ramp as indicated by the red rectangle. For simplicity we ignore the lateral dynamics of the vehicles and consider the model shown in Fig. 1(d). The distances of

the vehicles from the conflict zone are denoted by r_1 and r_2 while their longitudinal velocities are v_1 and v_2, respectively. The length of the conflict zone is denoted by L, the length of both vehicles is l, and we define $s \coloneqq L + l$.

By neglecting the air and rolling resistance, the longitudinal dynamics of the vehicles can be given by

$$\begin{aligned} \dot{r}_1 &= -v_1, \\ \dot{v}_1 &= u_1, \\ \dot{r}_2 &= -v_2, \\ \dot{v}_2 &= u_2, \end{aligned} \tag{1}$$

where the dot represents the derivative with respect to time t, and u_1 and u_2 represent the control inputs (i.e., acceleration commands) assigned to the vehicles. Note that the negative signs appear since the vehicles are traveling towards the negative direction. The velocity and acceleration values are constrained within the limits $v_1 \in [v_{\min,1}, v_{\max,1}]$, $v_2 \in [v_{\min,2}, v_{\max,2}]$, $u_1 \in [a_{\min,1}, a_{\max,1}]$, and $u_2 \in [a_{\min,2}, a_{\max,2}]$. We assume that these limits are known to the ego vehicle 2. Table 1 summarizes all parameter values used that correspond to typical highway driving. Notice that $v_{\min,2}$ is set to zero, meaning the merging vehicle is allowed to stop along the ramp if necessary.

Table 1 – Parameters values used in the paper

L	l	$a_{\min,1}$	$a_{\min,2}$	$a_{\max,1}$	$a_{\max,2}$	$v_{\min,1}$	$v_{\min,2}$	$v_{\max,1}$	$v_{\max,2}$
20 [m]	5 [m]	-4 [m/s^2]	-4 [m/s^2]	2 [m/s^2]	2 [m/s^2]	20 [m/s]	0 [m/s]	35 [m/s]	35 [m/s]

As mentioned before, when designing the decision making and control strategies for the ego vehicle 2, the status sharing messages are used, which contain the current status of the remote vehicle 1 (r_1 and v_1). We define the initial time to be the time when the first status packet is received by the ego vehicle 2. Notice that the remote vehicle 1 shares its motion information via V2X communication but we do not have control over its motion. Thus, one can only assign the input u_2 but does not have knowledge about the exact value of u_1 (except for its limits). With these, our goal is to ensure via u_2 that the vehicles do not appear in the conflict zone at the same time.

3. Conflict analysis

In this section, we review the conflict analysis originally proposed in [12]. Specifically, we use conflict chart as a tool to determine whether conflicts can be prevented for a given state, which can be used for decision making and control design for the ego vehicle.

A conflict is defined by both vehicles being (even partially) in the conflict zone at the same time, i.e., $\exists t, r_1(t) \in [-s, 0] \wedge r_2(t) \in [-s, 0]$; recall that s is the sum of conflict zone length and vehicle length. To ensure a non-conflicting maneuver, we introduce the following two propositions:

$$\begin{aligned} P &\coloneqq \{\exists t, r_1(t) = 0 \wedge r_2(t) < -s\}, \\ Q &\coloneqq \{\exists t, r_1(t) = -s \wedge r_2(t) > 0\}, \end{aligned} \tag{2}$$

where $\wedge$ denotes the logical conjunction “AND”. The proposition P suggests that the ego vehicle 2

merges ahead of remote vehicle 1 without a conflict (see Fig. 1(a)), while proposition Q implies that vehicle 2 merges behind vehicle 1 without a conflict (see Fig. 1(b)). One can show that

$$P \vee Q \iff \text{no conflict occurs,} \tag{3}$$

where $\vee$ is the logical disjunction "OR". In other words, to ensure a non-conflicting merge we need to ensure a conflict-free merge ahead or a conflict-free merge behind. We remark that this can be generalized to multiple-vehicle cases by considering pairwise conflicts and can be extended to many other traffic scenarios involving potential conflicts, e.g., unprotected left-turns, lane changes, etc.

One can further decompose proposition P (vehicle 2 merging ahead) into three cases:

(i) No-conflict case: vehicle 2 is able to merge ahead without conflict independent of the motion of vehicle 1;

(ii) Uncertain case: vehicle 2 may be able to merge ahead without conflict depending on the motion of vehicle 1;

(iii) Conflict case: vehicle 2 is not able to merge ahead without conflict independent of the motion of vehicle 1.

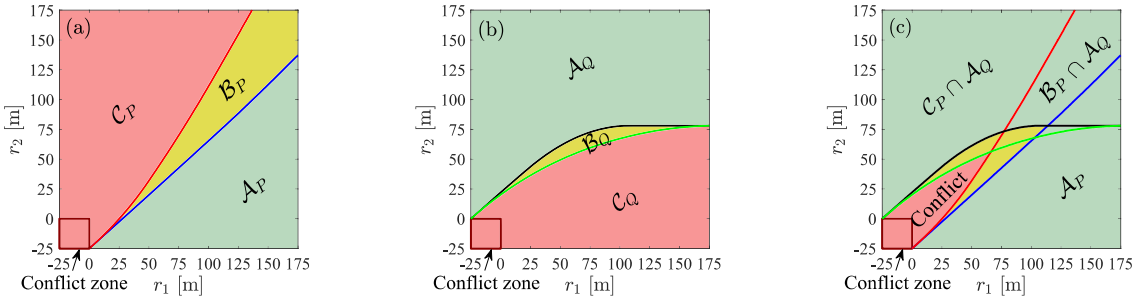

Fig. 2. - Conflict charts in the (r_1, r_2)-plane for $v_1 = 28$ [m/s] and $v_2 = 25$ [m/s]. (a) conflict chart for merge ahead, (b) conflict chart for merge behind, and (c) unified conflict chart. The dark red square with 25 [m] side length highlights the region where both vehicles are inside the conflict zone (even partially) at the same time.

These three cases correspond to three disjoint regions in the state space of the system (1), denoted by $\mathcal{A}_P$, $\mathcal{B}_P$, and $\mathcal{C}_P$, respectively; see [12] for detailed derivations. Fig. 2(a) shows these regions in the (r_1, r_2)-plane for velocities $v_1 = 28$ [m/s] and $v_2 = 25$ [m/s], where $\mathcal{A}_P$, $\mathcal{B}_P$, and $\mathcal{C}_P$ are shaded green, yellow, and red, respectively. By locating the current vehicle state on this chart, one can reason about conflict in terms of merge ahead, hence, this chart is called conflict chart. Similarly, proposition Q can be decomposed into no-conflict, uncertain, and conflict cases when merging behind instead of merge ahead. The corresponding regions in state space are denoted by $\mathcal{A}_Q$, $\mathcal{B}_Q$, and $\mathcal{C}_Q$, respectively. They are visualized in Fig. 2(b) with green, yellow, and red shadings.

The conflict charts for merging ahead and behind cases can be combined into a unified conflict chart as shown in Fig. 2(c), which is obtained by superimposing Fig. 2(a) and (b). We color the unified conflict chart using the following rules: superimposing a green region with any other region gives green;

superimposing a yellow region with a yellow or red region gives yellow; and superimposing two red regions gives red. Based on this, we can say that the green region is where a conflict can be prevented by the ego vehicle either merging ahead or behind the remote vehicle, while in the red region conflict is unavoidable. In the yellow region conflicts may or may not be prevented, depending on the motion of the remote vehicle. Notice that the boundaries separating these regions stretch far into the state space, enabling early decision making when the vehicles are far away from the conflict zone.

4. Decision making and control logic

In this section, we design decision making rule and control law for the ego vehicle using conflict charts. We focus on the green region in the unified conflict chart, since this is where a conflict is certainly avoidable by the ego vehicle, and thus, decisions of merge ahead and behind can be made. As shown in Fig. 2(c), the green region in the unified conflict chart can be divided into three sub-regions: the green region below the blue boundary ($\mathcal{A}_P$), the green region above the red boundary ($\mathcal{C}_P \cap \mathcal{A}_Q$), and the green region between the blue and red boundaries ($\mathcal{B}_P \cap \mathcal{A}_Q$). These three sub-regions correspond to three different decisions discussed below.

4.1 Merge ahead and merge behind regions

Based on the definition, in $\mathcal{A}_P$ region there is no conflict with respect to proposition P, i.e., the ego vehicle is able to merge ahead without a conflict independent of the motion of the remote vehicle. Thus, the decision for this region is indeed merge ahead; see Fig. 3(a) and the left part of the block diagram in Fig. 3(b). Merging ahead leads to higher time efficiency, and thus, has priority over merging behind. On the other hand, for the green region above the red boundary ($\mathcal{C}_P \cap \mathcal{A}_Q$), the ego vehicle is not able to merge ahead without conflict, but it is able to merge behind independent of the motion of the remote vehicle. Therefore, the ego vehicle decides to merge behind in this region; see Fig. 3(a) and (b).

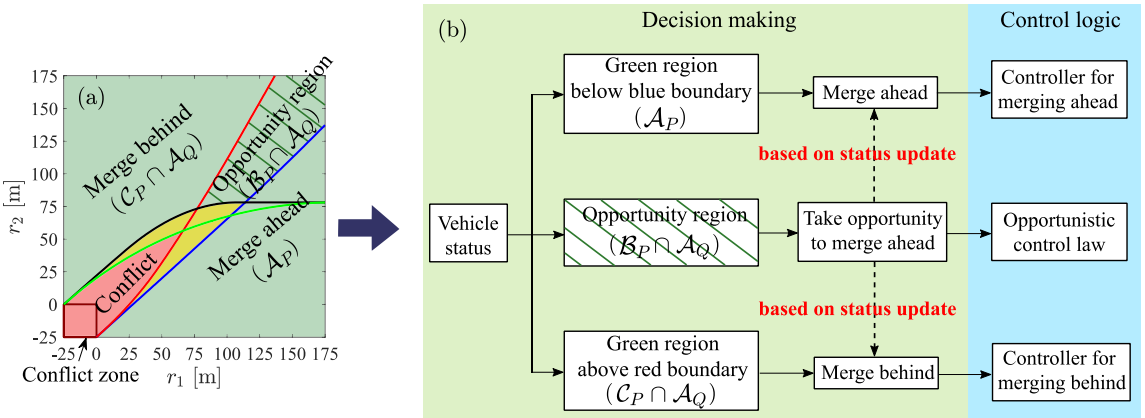

Fig. 3. - (a) Decision regions in the unified conflict chart. (b) Block diagram of the decision making and control for the ego vehicle 2.

In the two sub-regions discussed above, merge ahead and merge behind decisions can be made by the ego vehicle and can be executed by choosing appropriate control laws; see the right part of Fig. 3(b).

For example, the controllers proposed in [12] can be applied. They ensure conflict-free merge by keeping the evolution of the state inside the no-conflict regions $\mathcal{A}_P$ and $\mathcal{A}_Q$, respectively.

4.2 Opportunity region

Let us now look at the green region between the blue and red boundaries ($\mathcal{B}_P \cap \mathcal{A}_Q$), which is highlighted with stripes in Fig. 3(a). Here, merging ahead without conflict may be possible for the ego vehicle 2 depending on the future behavior of the remote vehicle 1, while merging behind without conflict is guaranteed independent of vehicle 1's future motion. Although a conservative decision for vehicle 2 is to merge behind, there exist potential opportunities of merging ahead without conflict which, if pursued, would benefit the ego vehicle's time efficiency. This striped region is called opportunity region, and we propose a strategy that enables the ego vehicle to pursue the opportunity of merging ahead, while still preventing conflict. To achieve this, a decision making rule and an opportunistic control law, which maximizes the ego vehicle's chance of merging ahead, are designed. In the meantime, we ensure conflict-free merge behind by keeping the state in the $\mathcal{A}_Q$ region when merging ahead is not possible.

The dashed arrows in Fig. 3(b) visualize the decision making of the ego vehicle in opportunity region, which is based on the status updates received from the remote vehicle via V2X. The ego vehicle can stick to the merge ahead decision if the state evolves into the region $\mathcal{A}_P$, that is, if the trajectory crosses the blue boundary in the conflict chart; see Fig. 3(a). On the other hand, the ego vehicles may decide to merge behind if the state evolves into the region $\mathcal{C}_P \cap \mathcal{A}_Q$, that is, if the trajectory crosses the red boundary in the conflict chart. Note that monitoring the state in conflict charts requires sustained V2X connectivity between the vehicles. As long as the state remains in the opportunity region, an opportunistic control law is applied; see the right part of Fig. 3(b). This "pushes" the system toward the blue boundary, i.e., toward the region $\mathcal{A}_P$, while keeping it inside the no-conflict region $\mathcal{A}_Q$.

By solving an optimization problem, one can prove that $u_2(t) \equiv a_{\max,2}$ is the input that pushes the state of the system toward the $\mathcal{A}_P$ region independent of vehicle 1's motion (although whether and when the state can enter $\mathcal{A}_P$ region still depends on vehicle 1's motion). Thus, the maximum acceleration $a_{\max,2}$ should be used as long as the state is inside the $\mathcal{A}_Q$ region. On the other hand, if the vehicle reaches the black boundary, the minimum acceleration $a_{\min,2}$ should be applied in order to keep the state within the $\mathcal{A}_Q$ region. That is, the control law can be summarized as follows

$$u_2^*(t) = \begin{cases} a_{\max,2}, & \text{if } t < t^*, \\ a_{\min,2}, & \text{otherwise,} \end{cases} \tag{4}$$

where t^* is the predicted time when the system state reaches the black boundary (see Fig. 3(a)) based on the latest status sharing packet. This time is predicted by considering the worst-case scenario for vehicle 1's motion ($u_1(t) \equiv a_{\min,1}$) in order to ensure the state always remains inside $\mathcal{A}_Q$ region independent of the future motion of vehicle 1. Note that the value of t^* can be updated as status updates are received, making the prediction less and less conservative.

If the state cannot enter the $\mathcal{A}_P$ region until t^*, meaning a decision change is not possible until the

predicted time when the state hits the black boundary, then we switch to a controller that keeps the state inside $\mathcal{A}_Q$ to guarantee a non-conflicting merge behind. In the worst-case scenario where vehicle 1 applies the minimal acceleration all along, only the control input $u_2(t) = a_{\min,2}$ manages to keep the state inside $\mathcal{A}_Q$. However, using status updates from the remote vehicle, less conservative input maybe used. If the state evolves into the $\mathcal{A}_P$ region, then the decision is changed to merge ahead and the ego vehicle may apply the maximum acceleration $a_{\max,2}$ to maximize its time efficiency. We remark that $a_{\max,2}$ and $a_{\min,2}$ are not necessarily the physical limits of vehicle 2, but are parameters that can be chosen by the users.

In summary, for states in the opportunity region, the decision making rule together with the opportunistic control law (4) enable the ego vehicle to safely pursue the opportunity of merging ahead.

5. Simulation with real highway data

In this section, we demonstrate the proposed decision making and control strategy by numerical simulations while using real highway data for the remote vehicle. We highlight the effectiveness of conflict charts as a tool to prevent conflicts.

For the remote vehicle, we use GPS data collected from a real human-driven vehicle approaching a merge zone on the US 23 highway near Ann Arbor, Michigan. The ego vehicle is assumed to be a connected automated vehicle merging from the on-ramp. Fig. 4(a) shows initial states A, B, and C (magenta crosses) in the conflict chart, which are located in the merge ahead region, opportunity region, and merge behind region, respectively. For all cases, the remote vehicle is initially at 150.68 [m] from the conflict zone traveling with a speed of 22.63 [m/s]. On the other hand, the ego vehicle is initially 120 [m], 147 [m], and 242 [m] away from the conflict zone traveling with a speed of 25 [m/s] for cases A, B, and C, respectively. We consider that the status sharing packet is received every 0.1 [s]. Fig. 4(b)-(d) show the trajectories of the system state (magenta crosses) by the time the ego vehicle exits the conflict zone, for the indicated initial states. It is confirmed that conflicts are prevented for all three cases since the trajectories never enter the conflict zone (i.e., the red square area in the conflict chart). In particular, for initial state B in the opportunity region, the ego vehicle successfully takes the opportunity of merging ahead.

The position, speed, and acceleration profiles are depicted in Fig. 4(e)-(g), where the data of the remote vehicle is shown in blue and the ego vehicle is distinguished by the black dashed, green, and black solid curves in cases A, B, and C, respectively. The red shaded area in Fig. 4(e) highlights the time when the remote vehicle occupies the conflict zone. For initial state A, the merge ahead decision is made and the maximum acceleration is used for the ego vehicle to merge ahead, which maximizes its time efficiency. For initial state B, the proposed strategy applies the maximum acceleration to pursue the opportunity of merging ahead, and eventually the system state enters the merge ahead region ($\mathcal{A}_P$) where the ego vehicle changes its decision to merge ahead. Finally, for initial state C, the ego vehicle successfully executes the merge behind decision by applying the corresponding controller while updating its acceleration as status updates are received; see the black solid curve in Fig. 4(f).

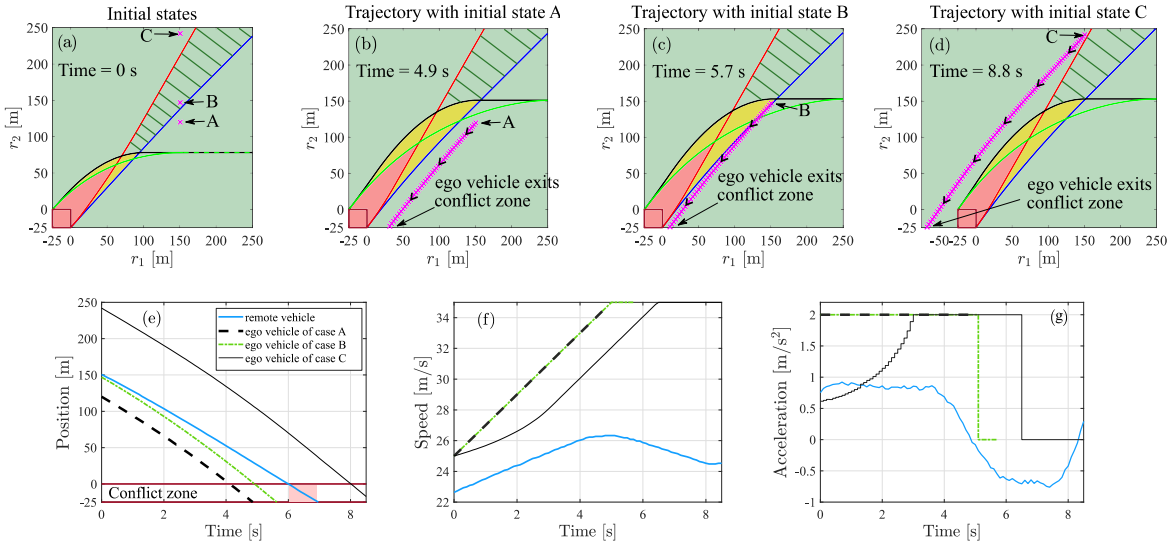

Fig. 4. - Simulation results with initial states in different decision regions when status sharing packets are received every 0.1 [s]. (a) initial states marked in conflict chart by magenta crosses indicating that the remote vehicle is 150.68 meters away from the conflict zone traveling with 22.63 [m/s], while the ego vehicle is 120 meters (Case A), 147 meters (Case B) and 242 meters (Case C) away from the conflict zone traveling with $v_2(0) = 25$ [m/s]. (b)-(d) trajectories for corresponding cases; (d)-(f): position, speed and acceleration profiles.

6. Conclusion

In this paper, we demonstrated that conflict charts are an effective tool to prevent conflicts in cooperative driving. A decision making and control strategy was proposed to guarantee a conflict-free highway merging maneuver by leveraging status update messages shared by a remote vehicle on the main road. The proposed strategy also improves time efficiency of the ego vehicle by minimizing the conservatism of its decision making. Using real highway data, we showed the effectiveness of the conflict charts-based strategy in terms of safety and time efficiency. Our future work includes scaling up the strategy design to a larger number of vehicles and different levels of cooperation.

References

1. Abboud, K., A. Omar, W. Zhuang (2016). Interworking of DSRC and cellular network technologies for V2X communications: A survey, *IEEE Transactions on Vehicular Technology,* vol. 65, no. 12, pp. 9457-9470.
2. Avedisov, S. S., G. Bansal, A. K. Kiss, G. Orosz (2018). Experimental verification platform for connected vehicle networks. In Proceedings *21st IEEE International Conference on Intelligent Transportation Systems (ITSC)*, Maui, USA, pp. 818-823.
3. Lehmann, B., H. J. Günther, L. Wolf (2018). A generic approach towards maneuver coordination for automated vehicles. In Proceedings *21st IEEE International Conference on Intelligent Transportation Systems (ITSC)*, Maui, USA, pp. 3333-3339.

4. Llatser, I., T. Michalke, M. Dolgov, F. Wildschütte, H. Fuchs (2019). Cooperative automated driving use cases for 5G V2X communication. In Proceedings *2nd IEEE 5G World Forum (5GWF),* Dresden, Germany, pp. 120-125.
5. Correa, A., S. Maerivoet, E. Mintsis, A. Wijbenga, M. Sepulcre, M. Rondinone, J. Schindler, J. Gozalvez (2018). Management of transitions of control in mixed traffic with automated vehicles. In Proceedings *16th International Conference on Intelligent Transportation Systems Telecommunications (ITST),* Lisboa, Portugal, pp. 1-7.
6. Medina, A. I. M., N. van de Wouw, H. Nijmeijer (2015). Automation of a T-intersection using virtual platoons of cooperative autonomous vehicles. In Proceedings *18th IEEE International Conference on Intelligent Transportation Systems (ITSC)*, Las Palmas, Spain, pp. 1696-1701.
7. Hafner, M. R., D. Cunningham, L. Caminiti, D. Del Vecchio (2013). Cooperative collision avoidance at intersections: Algorithms and experiments, *IEEE Transactions on Intelligent Transportation Systems,* vol. 14, no. 12, pp. 1162-1175.
8. Kianfar, R., P. Falcone, J. Fredriksson (2013). Safety verification of automated driving systems, *IEEE Intelligent Transportation Systems Magazine,* vol. 5, no. 4, pp. 73-86.
9. SAE J3216 (2020). Taxonomy and definitions for terms related to cooperative driving automation for on-road motor vehicles. SAE International, Tech. Rep.
10. Ge, J. I., S. S. Avedisov, C. R. He, W. B. Qin, M. Sadeghpour, G. Orosz (2018). Experimental validation of connected automated vehicle design among human-driven vehicles, *Transportation Research Part C*, vol. 91, pp. 335-352.
11. Avedisov, S. S., G. Bansal, G. Orosz (2021). Impacts of connected automated vehicles on freeway traffic patterns at different penetration levels, *IEEE Transactions on Intelligent Transportation Systems,* [Online]. Available: https://doi.org/10.1109/TITS.2020.3043323
12. Wang, H. M., T. G. Molnár, S. S. Avedisov, A. H. Sakr, O. Altintas, G. Orosz (2020). Conflict analysis for cooperative merging using V2X communication. In Proceedings *31st IEEE Intelligent Vehicles Symposium (IV)*, Las Vegas, USA, pp. 1538-1543.
13. SAE J2735 (2016). Dedicated short range communications (DSRC) message set dictionary set. SAE International, Tech. Rep.